Integrative Biology, 2019, 00(00), 1–11

doi: 10.1093/intbio/zyz008
Original Article

ORIGINAL ARTICLE

Microfluidic platform for studying osteocyte mechanoregulation of breast cancer bone metastasis

Xueting Mei[1,2,†], Kevin Middleton[2,†], Dongsub Shim[1], Qianqian Wan[1], Liangcheng Xu[2], Yu-Heng Vivian Ma[2], Deepika Devadas[1], Noosheen Walji[1], Liyun Wang[3], Edmond W.K. Young[1,2], and Lidan You[1,2,*]

[1]Department of Mechanical and Industrial Engineering, University of Toronto, Toronto, ON, Canada, [2]Institute of Biomaterials and Biomedical Engineering, University of Toronto, Toronto, ON, Canada, and [3]Department of Mechanical Engineering, University of Delaware

*Corresponding author. E-mail: youlidan@mie.utoronto.ca

Abstract

Bone metastasis is a common, yet serious, complication of breast cancer. Breast cancer cells that extravasate from blood vessels to the bone devastate bone quality by interacting with bone cells and disrupting the bone remodeling balance. Although exercise is often suggested as a cancer intervention strategy and mechanical loading during exercise is known to regulate bone remodeling, its role in preventing bone metastasis remains unknown. We developed a novel *in vitro* microfluidic tissue model to investigate the role of osteocytes in the mechanical regulation of breast cancer bone metastasis. Metastatic MDA-MB-231 breast cancer cells were cultured inside a 3D microfluidic lumen lined with human umbilical vein endothelial cells (HUVECs), which is adjacent to a channel seeded with osteocyte-like MLO-Y4 cells. Physiologically relevant oscillatory fluid flow (OFF) (1 Pa, 1 Hz) was applied to mechanically stimulate the osteocytes. Hydrogel-filled side channels in-between the two channels allowed real-time, bi-directional cellular signaling and cancer cell extravasation over 3 days. The applied OFF was capable of inducing intracellular calcium responses in osteocytes (82.3% cells responding with a 3.71 fold increase average magnitude). Both extravasation distance and percentage of extravasated side-channels were significantly reduced with mechanically stimulated osteocytes (32.4% and 53.5% of control, respectively) compared to static osteocytes (102.1% and 107.3% of control, respectively). This is the first microfluidic device that has successfully integrated stimulatory bone fluid flow, and demonstrated that mechanically stimulated osteocytes reduced breast cancer extravasation. Future work with this platform will determine the specific mechanisms involved in osteocyte mechanoregulation of breast cancer bone metastasis, as well as other types of cancer metastasis and diseases.

Keywords: microfluidics, bone metastasis, osteocytes, mechanical regulation, extravasation, breast cancer

Statement of Integration, Innovation and Insight

Bone metastasis is a severe complication that occurs in approximately 85% of patients with advanced breast cancer. The potential of exercise in attenuating metastatic tumor growth in bone had been shown *in vivo*. Osteocytes are

(*Continued*)

[†]Equal contributions.

Received November 9, 2018; **revised** January 27, 2019; **editorial decision** March 2, 2019; **accepted** May 2, 2019

(Continued)
identified regulators in mediating loading inhibited bone metastasis *in vitro*. However, there is no ideal platform currently available for investigating the impact and mechanism underlying loading reduced bone metastasis. To bridge the gap between *in vivo* and *in vitro* experiments, we developed a novel microfluidic cancer extravasation tissue platform that integrates stimulatory bone fluid flow and real-time bi-directional signaling between multiple cell populations.

INTRODUCTION

Bone metastasis is the process in which cancer cells detach from the primary tumor, circulate through the blood vessels, and extravasate to the bone. Approximately 85% of advanced breast cancer patients experience bone metastasis [1], due to the favorable 'soil' microenvironment in bone, which establishes a pre-metastatic niche for breast cancer cells [2]. As a dynamic organ, bone undergoes a lifelong remodeling process to maintain normal bone strength and function [3]. Metastasized breast cancer cells disrupt the normal remodeling process by interacting with both osteoblasts (bone-formation cells) and osteoclasts (bone-resorption cells) [4], as well as osteocytes (ubiquitous bone cells embedded in the bone matrix) [5]. This results in symptoms such as reduced bone quality, bone fractures, severe pain, and significantly reduced survival rates [4]. Therefore, prevention of bone metastasis is critical in improving advanced breast cancer patient outcomes.

While bone metastasis cannot be cured, surgery, chemotherapy, hormone, and radiation therapy can be used to slow its progression [6]. However, these treatments have many adverse side effects. Exercise is often suggested for patients after chemotherapy to improve fitness, muscle strength, and walking speed. Furthermore, clinical and *in vivo* studies demonstrated that exercise also reduced the rate of adverse skeletal events as well as tumor formation [7, 8]. However, no clinical study has been performed investigating the role of mechanical loading on bone due to exercise in preventing bone metastasis.

Since bone metastasis is a complex process which requires a favorable 'soil' at the secondary site, researchers have studied the interaction between breast cancer cells and multiples cell types within the bone matrix. It has been demonstrated that osteolytic bone metastasis starts a vicious cycle whereby osteoclast-initiated bone degradation and resorption increase. This results in the release of bone-derived factors embedded in the bone matrix [9], such as transforming growth factor beta (TGF-β), insulin-like growth factor (IGF), and osteoclast lipid secretions that further promotes cancer extravasation. Although the majority breast cancer bone metastasis is osteolytic, lesions can also be osteoblastic, where increased osteoblast activity and bone formation is mediated by tumor-secreted endothelin-1 [10]. Other than bone cells, another major regulator of bone metastasis is the endothelium of the metastatic site, which is the barrier that cancer cells need to extravasate through to reach the bone environment [11]. Consequently, many studies focus on the role of endothelium permeability and surface adhesion molecules [12–15] in cancer extravasation.

Osteocytes, however, have only recently been investigated for their role in bone metastasis [5, 16–19] despite being a major regulator of osteoblast, osteoclast, and endothelial activity [20–25]. Osteocytes sense the shear stress caused by interstitial fluid flow from bone loading during exercise [26]. Through mechanotransduction, mechanically stimulated osteocytes have modulated expression of signaling molecules that regulate the recruitment and activity of osteoclasts and osteoblasts [25–27], and thus regulate the bone remodeling process [28]. Furthermore, our recent *in vitro* studies demonstrated that mechanically stimulated osteocytes regulated breast cancer migration via both direct signaling to cancer cells and indirect signaling mediated by both osteoclasts and endothelial cells [18, 19].

In vivo models have been developed to study bone metastasis. Despite greater physiological relevance, *in vivo* experiments are expensive, time consuming, and difficult to control for specific factors. Conversely, most macro-scaled *in vitro* experiments only provide 2D cell culture environments and often lack real-time cell-cell signaling between different cell populations. To bridge this gap, microfluidic metastasis models have been established to replicate the physiological endothelium [29, 30] and bone microenvironments [31, 32]. Recent studies have developed physiologically relevant tissue models of the blood vessel environment through which the cancer cell extravasates, and attempt to mimic the secondary tumor environment [33–35]. In the case of bone metastasis, microfluidic devices have been developed to model the bone environment containing osteodifferentiated mesenchymal stem cells embedded in collagen gel [31, 32] or in a native bone matrix with perfusion flow [36]. Although these models provide excellent platform to study various important aspects of bone metastasis, the mechanical regulation of bone metastasis via major bone mechanosensing cell population, osteocytes, cannot be investigated [17, 18].

In this study, we present the first microfluidic tissue model for bone metastasis that is capable of applying physiologically relevant mechanical stimuli to osteocytes. This model consists of a simulated blood vessel environment with endothelial cells coating a 3D lumen structure through which cancer cells can extravasate, and a model bone environment that can apply physiologically relevant mechanical forces to cells. This microfluidic model was utilized to determine the effects of mechanically stimulated osteocytes on the extravasation of breast cancer cells (Fig. 1). This model can be used to study other cancer types that typically metastasize to the bone, such as prostate cancer, or be applied to other tissue models of diseases that typically undergo mechanical stimulation, such as in the lung. Furthermore, this model could be utilized in drug studies to identify their effects in a more controlled and physiologically relevant mechanical microenvironment.

MATERIALS AND METHODS

Cell culture

MLO-Y4

MLO-Y4 cells (a gift from Dr. Lynda Bonewald, Indiana University) were used as an osteocyte model. The cells were maintained in tissue culture-treated petri dishes coated with Type-I collagen (0.15 mg/ml rat-tail Collagen-I (Corning, USA) in 0.02 N Acetic Acid (Sigma-Aldrich, USA)), and were grown in

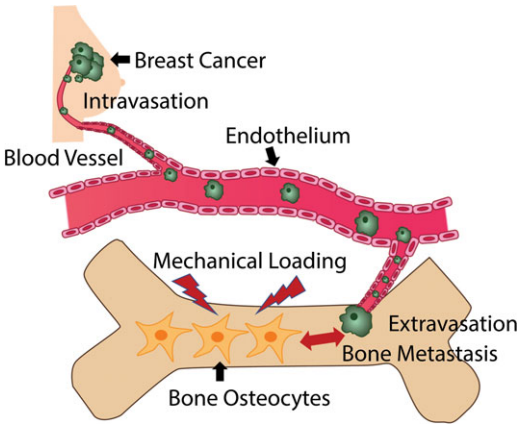

Figure 1 Bone metastasis process of breast cancer. Cancer cells break off from the primary tumor and intravasate into the blood stream. Next, the cells adhere to the endothelium and can extravasate towards the bone environment. We believe mechanical loading of the osteocytes can regulate this extravasation process.

MLO-Y4 medium (94% v/v α-MEM (Wisent, Canada), 2.5% fetal bovine serum (FBS, Gibco, USA), 2.5% calf serum (CS, Thermo Fisher, USA), 1% penicillin streptomycin (P/S, Gibco, USA)). The MLO-Y4 cells were grown to 80% confluence, at which point they were detached with Trypsin-EDTA (Gibco, USA), and passaged up to passage 35 at 2–3 × 10^5 cells per dish.

RAW264.7

The RAW264.7 cell line (ATCC, USA) was differentiated into osteoclasts and used to produce osteoclast conditioned medium (OCL CM). The cells were cultured on tissue culture-treated petri dishes in RAW264.7 medium (87% v/v DMEM (Sigma-Aldrich, USA), 10% FBS (Gibco, USA), 2% L-Glutamine (Gibco, USA), and 1% P/S). The cells were passaged every 3 days up to passage 14 by removing the cells from the dish using a cell scraper and re-seeded at 500k cells per dish.

For osteoclastogenesis, RAW264.7 cells were seeded in RAW264.7 medium supplemented with 50 ng/ml RANKL (Cedarlane, Canada) and grown for 6 days. On day 7, the media was switched to RAW264.7 medium. The media was then collected after one day as OCL CM. Differentiation was validated by staining for tartrate resistant acid phosphatase (TRAP) [17] with a TRAP-staining solution (5 mg Naphthol AS-MX phosphate (Sigma-Aldrich, USA), 250 µl Ethylene Glycol Monoethyl Ether (Sigma-Aldrich, USA), 50 ml TRAP buffer (0.68 g 100 mM Sodium Acetate Trihydrate (Thermo Fisher, USA), 0.58 g L(+) Tartaric Acid (Sigma-Aldrich, USA), 0.1 ml 99.5% Acetic Acid in DI water), 30 mg Fast Red Violet LB Salt (Sigma-Aldrich, USA)).

MDA-MB-231

MDA-MB-231 cells (ATCC, USA), a metastatic breast cancer cell line, were grown in T-75 flasks in MDA media (F-12K (Gibco, USA) with 10% FBS and 1% P/S). The cells were passaged every 3 days to passage 25 by trypsinizing the cells, and re-seeding at 5 × 10^5 cells per flask.

HUVEC

HUVEC's (a gift from Dr. Craig Simmons, University of Toronto) were used to generate vessel-like structures. They were maintained in T-75 flasks in HUVEC media (EndoMax base media (Wisent, Canada) with 10% FBS, 2% Wisent Supplement (Wisent, Canada), 1% P/S) until passage 10. The cells were passaged every week by first removing the cells from their flask with Trypsin-EDTA, and re-seeding them at 5 × 10^5 cells per flask.

Pump Design

To generate oscillatory fluid flow (OFF) with a peak shear stress of 1 Pa and frequency of 1 Hz, we made a custom microfluidic pump (Fig. 2A), which consists of a stepper motor (Polalu, USA) controlled by a microcontroller (Arduino, Italy) and a stepper motor driver (ITEAD, China). The pump is used to compress and release, in an oscillating fashion, a compliant tube attached to a microfluidic device. This generates a pressure gradient along the length of the channel, which produces fluid flow and shear stresses within the device. A numerical model was developed in MATLAB (MathWorks, USA) to determine microfluidic pump and device parameters to generate physiologically relevant shear stresses (0.8–5 Pa for osteocytes [37–39]). Specific details on the numerical model can be found in supplement S1.

Pump validation

The shear stresses generated by the pump were measured through particle image velocimetry (PIV). A cell suspension (1 M cells/ml) was loaded into a single microfluidic channel, and the pump was used to generate fluid flow. The flow was recorded at 30 FPS using a microscope camera (Canon, Japan). Frame by frame displacements of cells in the fluid were measured in ImageJ (NIH, USA), and were used to calculate the average fluid velocity and flow rate, Q, which was applied to estimate the wall shear stresses, τ_{wss}, with equation (1).

$$\tau_{wss} = \frac{6Q\mu}{h^2 w} \tag{1}$$

Where μ is the fluid dynamic viscosity, h is the channel height, and w is the channel width.

Calcium imaging experiments were performed to validate that flow generated from the pump could stimulate a mechanoresponse in osteocytes seeded in a microfluidic channel similar to what is observed in well-established osteocyte mechanobiology experiments [40]. MLO-Y4 cells were seeded in the osteocyte (OCY) channel of a device on collagen I (Fig. 2B), or on glass slides coated with collagen I for parallel plate flow chamber (PPFC) controls. The cells were grown to 80% confluence and stained with Fura-2 AM (Ex: 340 nm/380 nm, Em: 510 nm; Thermo Fisher, USA). The stain was prepared by reconstituting 50 µg of Fura-2 AM in 50 µl of DMSO (Sigma-Aldrich, USA) and diluting in 5 ml of working media (97% α-MEM without phenol red, 1% FBS, 1% CS, and 1% P/S). The cells were washed with DPBS, and the stain was applied to the cells for 45 minutes at room temperature in darkness. The cells were rinsed with DPBS and loaded with working media. The device was connected to the pump (microfluidic or syringe pump (for the PPFC)) and placed on the microscope for at least 30 minutes before the experiment began to normalize the osteocyte mechanosensitivity. Cells were imaged using EasyRatioPro (PTI, USA). For the first 1–2 minutes a static baseline reading of cell response was taken, after which 2–3 minutes of flow (1 Pa, 1 Hz) was applied to the osteocytes. After the experiment, the calcium data (340 nm/380 nm ratio) was analyzed using a previously developed MATLAB script [41]. A significant intracellular calcium response was taken as at least twice the maximum baseline peak.

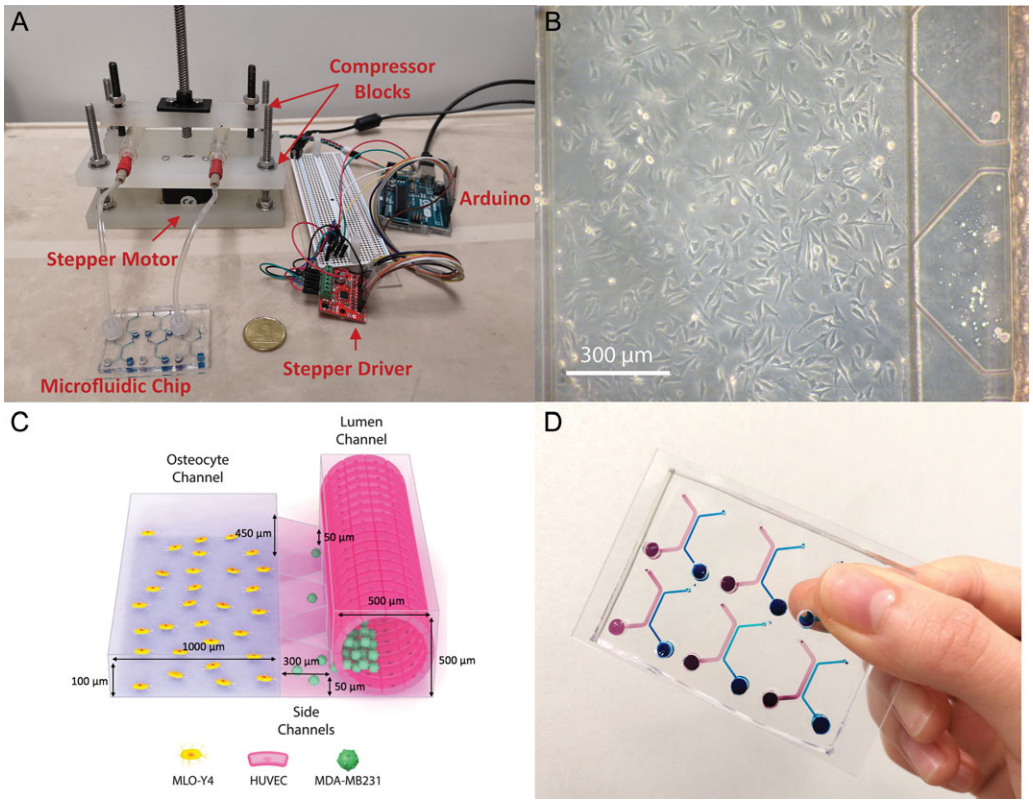

Figure 2. (A) Microfluidic pumping system consisting of stepper motor controlled by an Arduino microcontroller and a stepper driver that compresses gas-filled tubing connected to a microfluidic chip. Loonie for scale. (B) MLO-Y4 osteocytes seeded in microfluidic channel. (C) 3D representation of microfluidic device with osteocytes seeded within the OCY channel, breast cancer cells seeded within an endothelial lumen in the lumen channel, and side channels that the breast cancer cells invade into. (D) Microfluidic chip with six microfluidic devices arrayed. OCY channel is dyed purple and the lumen channel is dyed blue.

Microfluidic device fabrication

A two-channel microfluidic device (Fig. 2C) was fabricated to model osteocyte mechanoregulation of breast cancer extravasation (specific channel dimensions are provided in Fig. 2C). A negative multi-layered silicon SU-8 master was produced using SU-8 2050 and 2075 (Microchem, USA) to prepare the osteocyte and side channel layers, and the lumen channel respectively by following standard photolithography procedures [42]. Polydimethylsiloxane (PDMS) elastomer base and curing agent (Dow Corning, USA) were mixed at a 10:1 ratio, degassed for 1 hour, poured on top of the master, and baked at 80°C for 4 hours. The PDMS devices were plasma treated for 1.5 minutes and bonded to a glass slide to form the microfluidic chip (Fig. 2D). The microfluidic chip was arrayed to increase fabrication and experimental throughput. Devices were used on the same day of bonding.

Lumen fabrication

The channels were sterilized by incubating in 70% ethanol for 10 minutes, and then washed with DPBS three times. 100 µg/ml fibronectin solution (Sigma-Aldrich, USA) diluted in DPBS was used to coat the microchannels for 40 minutes. A hydrogel mixture of collagen gel (50 µl 5X DPBS (Sigma-Aldrich, USA), 0.78 µl of 5.0 N NaOH (Sigma Aldrich, USA), 195 µl of 9.59 mg/ml Type I rat tail collagen (Corning, USA)) and Matrigel® (Corning, USA)), with final concentrations of 5.5 mg/ml and 2.5 mg/ml respectively, was prepared. The hydrogel mixture was pipette-loaded to fill the entire lumen channel, and aspirated after 30 seconds to form the lumen. Finally, the microchannels were incubated at 37°C in a water bath for 45 minutes before adding in media.

Lumen validation

The lumen shape and integrity were validated by coating the lumen walls with 1.0 µm blue fluorescent microspheres (Ex: 365 nm, Em: 415 nm, Invitrogen, USA). The lumens were imaged using a confocal microscope (Nikon, Japan). Similarly, to ensure that endothelial cells could survive and form a physiological barrier to cancer cell migration, HUVECs were pipette-loaded into the hydrogel lumen at a density of 2×10^6 cells/ml per side. To coat all circular sides of the lumen, the cells were loaded and the channel was positioned so the cells would attach to one portion of the channel at a time as previously described [43]. The cells were incubated at 37°C for at least 6 hours to reach confluence and form intercellular connections. Media for the cells was replaced every 24 hours for up to 78 hours. The cells were characterized in the lumen at either 6 or 78 hours using confocal microscopy. To prepare the cells for imaging, the cells were fixed with 10% formalin (Sigma-Aldrich, USA), stained with DAPI (Ex: 364 nm, Em: 454 nm; Cell Signaling Technology, USA) to image the cell nucleus, and then stained with a VE-cadherin primary antibody (Abcam, UK) and a secondary antibody conjugated to Alex Fluor™ 488 (Ex: 488 nm, Em: 520 nm; ThermoFisher, USA).

To demonstrate that bone residing cell released signals could diffuse between channels, a 40 kDa FITC conjugated

dextran (Ex: 490 nm, Em: 520 nm; Sigma-Aldrich, USA) was used as a model of VEGF, a potent regulator of endothelial function that is also expressed by osteocytes [20, 21]. An acellular hydrogel lumen was prepared in the microfluidic device with DPBS added to the lumen. The FITC dextran solution (1 mg/ml in DPBS) was added to the 'OCY channel, and the lumen was imaged at discrete time points using a fluorescent microscope (Nikon, Japan). After the experiment, the images were analyzed using ImageJ to quantify the fluorescent intensity along the width of the hydrogel filled side channel and lumen. All intensities were normalized to the value obtained at the interface between the lumen channel and the side channel.

Experimental design

Group I—validation

As a proof of concept experiment, the ability of the device in allowing cellular signaling and facilitating extravasation response was validated by confirming the effect of osteoclast-released factors, a known stimulator of breast cancer bone metastasis [44], on cancer cell extravasation. Specifically, MLO-Y4 osteocytes were seeded in the OCY channel in either MLO-Y4 media or a 1:1 mixture of MLO-Y4 media and OCL CM. Acellular controls were prepared with only MLO-Y4 media added to the OCY channel. The devices were incubated overnight, and an endothelial lumen was prepared with HUVECs stained with CellTracker™ Red (Ex: 577 nm, Em: 602 nm; Invitrogen, USA). After 6 hours, MDA-MB-231 cells stained with CellTracker™ Green (Ex: 492 nm, Em: 517 nm; Invitrogen USA) were seeded on the lumen side adjacent to the side channels, and the cells were provided a 1:1 mixture of HUVEC and MDA-MB-231 media. The side channels were imaged every 24 hours using fluorescent microscopy. Media in both channels were replaced every 24 hours.

Group II—extravasation while osteocytes under flow in the OCY channel

To study the impact of mechanically stimulated osteocytes on breast cancer extravasation, MLO-Y4 osteocytes were seeded in the OCY channel and either underwent daily fluid stimulation (1 Pa, 1 Hz) for 2 hours for the first 2 days of the experiment, or were kept static. The endothelial lumen channel was kept static under all circumstances. Acellular controls were again prepared as above. The lumen channel was prepared by seeding HUVECs and MDA-MB-231 cells as described above. The side channels were fluorescently imaged and media was replaced every 24 hours.

Group III—extravasation while flow in the unseeded OCY channel

To investigate whether the integration of fluid flow in the OCY channel affect breast cancer extravasation, channels were prepared as above in Group II, but with no osteocytes seeded in the OCY channel. The OCY channel was exposed to fluid flow as described above, or was kept static for the experiment duration. The endothelial lumen channel was again kept static under all circumstances. The side channels were again fluorescently imaged every 24 hours.

Different experimental conditions are summarized in Table 1.

Statistics

All statistical analysis was performed using RStudio® (RStudio, USA). The calcium results were analyzed by comparing the percentage of responding cells and the mean magnitude of that response in the microfluidic device and the PPFC. Statistical significance was assessed by performing the student's t-test.

In the extravasation experiments, each side channel was quantified in terms of 1) extravasation distance and 2) the percentage of extravasated side channels out of all the side channels in the device. Cancer cell extravasation distance was quantified by measuring the average change in position of MDA-MB-231 cells (green fluorescent stained cells) from the hydrogel boundary at 24 hours and 72 hours using ImageJ. The percentage of extravasated side channels was determined by counting the number of side channels with at least one breast cancer cell and dividing it by the total number of side channels on the device. Furthermore, duplicate conditions on the same microfluidic chip and/or in the same incubator were also averaged together. For Group I and II experiments, both extravasation distance and extravasation percentage were normalized to acellular controls on the same microfluidic chip and/or in the same incubator. All results were paired with experimental conditions performed simultaneously on the same microfluidic chip and/or in the same incubator. Statistical analysis of the extravasation data was performed with paired *t*-tests. For all experiments, the Holm-Bonferroni method was applied for multiple comparisons, and statistical significance was taken at $\alpha = 0.05$.

RESULTS

Microfluidic pump validation

The numerical model was developed to calculate the shear stress within the microfluidic device, which is compared to the shear stress calculated by the velocity measured by PIV in the device given different pump parameters (Fig. 3A). Both the model and experimental results demonstrated that physiological wall shear stresses could be generated using this pump. This pump was also able to stimulate calcium responses in osteocytes (Fig. 3B), which were not significantly different than those produced using a PPFC in terms of percentage of responding

Table 1. Extravasation conditions.

Experiment	Condition	MLO-Y4 Media	OCL CM	MLO-Y4 Cells	Flow in OCY channel
Group I	Acellular Control	100%	-	–	–
	MLO-Y4	100%	-	+	–
	MLO-Y4 + OCL CM	50%	50%	+	–
Group II	Acellular Control	100%	-	–	–
	MLO-Y4	100%	-	+	–
	MLO-Y4 + Flow	100%	-	+	+
Group III	Static	100%	-	–	–
	Flow	100%	-	–	+

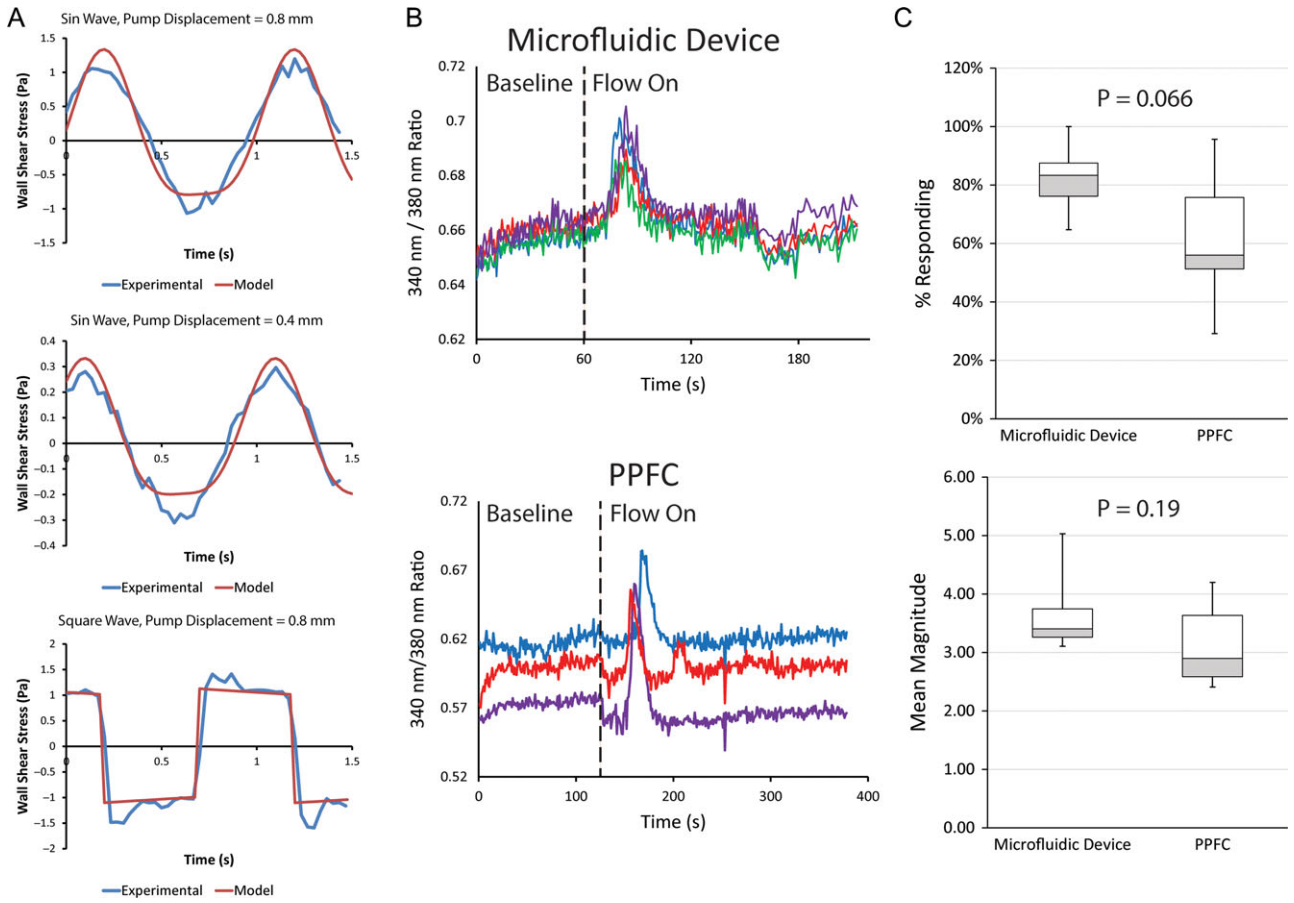

Figure 3. (A) Comparison of experimental (blue lines) and model (red lines) predicted wall shear stresses in the microfluidic device using different pumping parameters. (B) Typical osteocyte calcium responses obtained within the microfluidic device and PPFC. Representative calcium response curves in multiple different osteocytes were presented in the lower panel. Dotted black lines designate time when flow was turned on. (C) Box plots comparing the percentage and mean magnitude of calcium response in the microfluidic device and the PPFC. $N = 5$ for the microfluidic device and $N = 11$ for the PPFC.

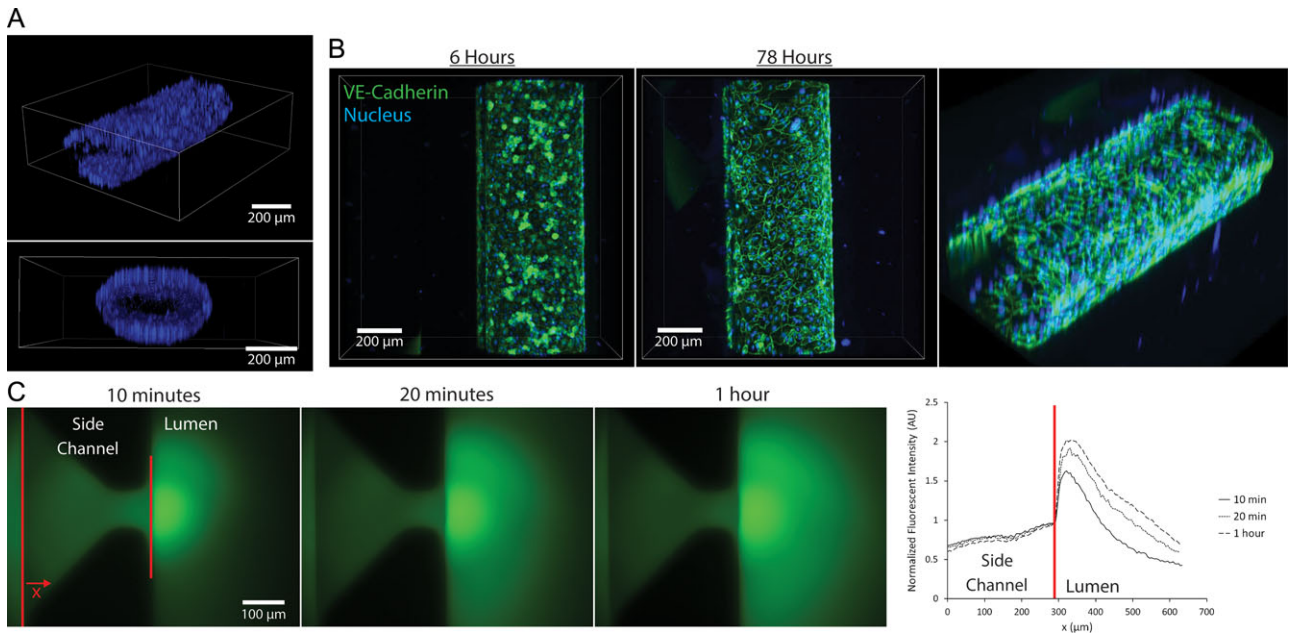

Figure 4. (A) Isometric and front view of lumen in microfluidic device coated on all sides with fluorescent microbeads. (B) VE-cadherin (green) and DAPI nuclear staining (blue) of HUVECs seeded within a microfluidic lumen at 6 hours and 78 hours after initial seeding. Also includes the isometric view of a HUVEC containing lumen at 78 hours. (C) Images at different time points of FITC conjugated dextran dye diffusing from the OCY channel (left) into the acellular hydrogel lumen (right). As well, plot of fluorescent intensities measured along the width of the side channel into the lumen channel at different time points. Fluorescent intensities are normalized to the interface between the side channel and the lumen channel. The red 'x' designates x = 0 μm on the plot, and the red bar on the right designates the point of normalization for comparing plots.

cells (82.3% vs. 61.7%) and mean response magnitude of responding cells (3.71 vs. 3.13 times baseline) (Fig. 3C).

HUVEC seeded microfluidic lumen validation

The lumen was uniformly ellipsoidal in shape along its length (Fig. 4A). HUVECs were also able to achieve confluence and produce VE-cadherin intercellular connections 6 hours after seeding within the lumen (Fig. 4B). These intercellular junctions were able to be maintained for the entire 78 hours of the experiment (Fig. 4B). As well, the acellular hydrogel lumen permitted diffusion of dextran with similar molecular weights to many regulatory signals (e.g. VEGF, RANKL) [45, 46] (Fig. 4C).

Extravasation of breast cancer cells to the bone environment

Group I—validation

We validated that this platform can stimulate cancer cell extravasation towards signals secreted by osteoclasts. Supplementation of OCL CM to the MLO-Y4 cells induced a significant increase in extravasation distance compared to just MLO-Y4 cells (134.5 μm vs. 63.8 μm, or 72.4% vs. 31.3% of the control distance) (Fig. 5A). However, no difference was observed in terms of the percentage of extravasated side channels (non-normalized 60.0% for MLO-Y4 cells with OCL CM vs. 55.7% for just MLO-Y4 cells, or 66.1% for MLO-Y4 cells with OCL CM vs. 57.9% for just MLO-Y4 cells normalized to control) (Fig. 5A).

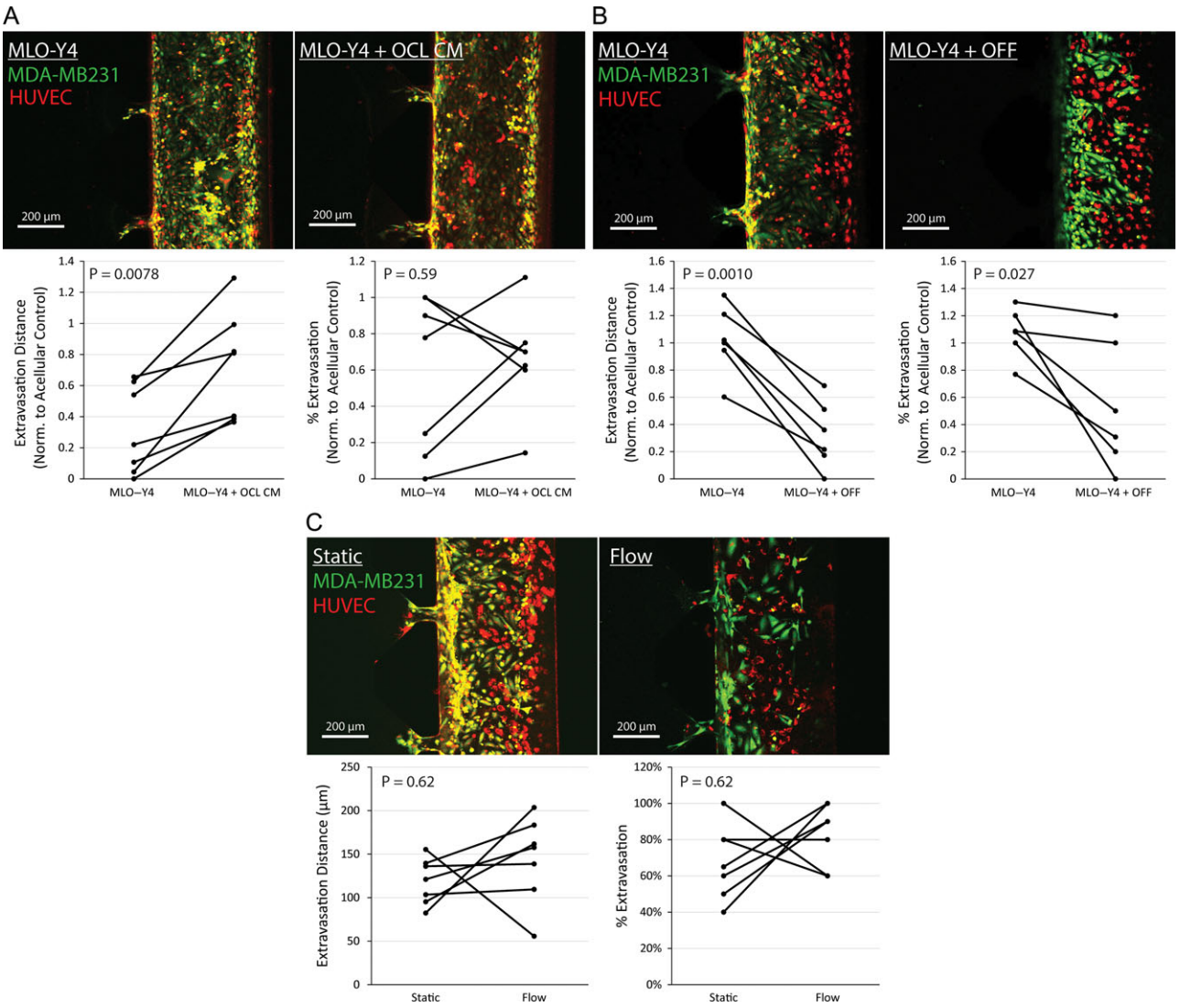

Figure 5. (A) Group I experiment: representative fluorescent images of breast cancer cells (green) extravasating through the endothelial cell lumen (red) into the side channel when exposed to signals from just MLO-Y4 cells, or MLO-Y4 cells supplemented with OCL CM. Plots comparing the extravasation distance and percentage of extravasated side channels of pairs of both conditions. N = 7 pairs. (B) Group II Experiment: Fluorescent images of MDA-MB-231 cells extravasating into side channels given signals from MLO-Y4 cells or MLO-Y4 cells exposed to OFF mechanical stimulation. Plots comparing the extravasation distance and percentage of extravasated side channels of pairs of both conditions. N = 6 pairs. (C) Group III Experiment: Fluorescent images of MDA-MB-231 cells extravasating into side channel in devices that undergo no flow, or flow. Plots comparing breast cancer cell extravasation distance and percentage of side channels extravasated into side channels. N = 7 pairs.

Group II—extravasation while osteocytes under flow in the OCY channel

To investigate the regulation of breast cancer extravasation by osteocytes under flow, we compared cancer cell extravasation when osteocytes were stimulated with fluid shear stresses to unstimulated osteocytes. We observed a significant reduction in extravasation distance in the OFF condition (36.6 μm, or 32.4% of the control) compared to the static osteocytes (110.3 μm, or 102.1% of the control) (Fig. 5B). In terms of the percentage of side channels extravasated, there was also a significant decrease when OFF was applied to the MLO-Y4 cells (33.8% non-normalized, or 53.5% of the control) compared to without (67.2% non-normalized, or 107.3% of the control) (Fig. 5B).

Group III—extravasation with flow in the unseeded OCY channel

Finally, to investigate whether the observed difference in extravasation in the group II experiment is due to flow-induced mechanical property gradients (e.g. pressure) across the side channels, we quantified the extravasation of breast cancer cells in response to acellular OCY channels exposed to flow or no-flow. We observed no significant difference between the application of flow or no-flow on both extravasation distance (144.3 μm and 119.0 μm respectively) and the percentage of extravasated side channels (82.9% and 67.9% respectively) (Fig. 5C).

DISCUSSION

Metastasis of breast cancer to the bone is a serious condition, which significantly reduces the quality of life and worsens prognosis in patients. Clinical and *in vivo* studies have shown that exercise may have positive effects on patients with bone metastasis [7, 8] and, more specifically, our recent *in vitro* study suggested an impact of mechanical loading of bone cells on preventing breast cancer extravasation [18]. Despite these findings, currently there is no microfluidic tissue platform to investigate the impact of exercise on breast cancer bone metastasis through osteocyte mechanoregulation. Therefore, we developed a novel microfluidic tissue platform that provides a physiologically relevant mechanical bone cell microenvironment for studying the breast cancer cells extravasation, allows for real-time intercellular communication between different cell populations, and integrates stimulatory bone fluid flow at physiological levels.

Using our platform, we observed an increase in extravasation distance of the cancer cells in the presence of OCL CM, but no significant effect on the percentage of side channels extravasated (group I) (Fig. 5A). Osteoclasts are known to stimulate cancer metastasis by both the breakdown of bone matrix (thereby releasing growth factors), and the direct secretion of osteoclast signals [9]. In the absence of bone matrix resorption, studies have shown that deproteinized OCL CM and lipids extracted from OCL CM promote cancer migration through the up-regulation of arachidonic acid and the down-regulation of lysophosphatidylcholine [44]. In addition, sphingosine 1 phosphate (S1P) is secreted by osteoclasts [47], and is known to promote breast cancer migration [48] by upregulating matrix metalloproteinase (MMP)-9 [49], which breast cancer cells utilize to degrade extracellular matrix (ECM). However, S1P also has the ability to enhance endothelial integrity [50], thereby inhibiting the extravasation of breast cancer cells. It is likely that the extravasated MDA-MB-231 cancer cells extravasated farther via increased matrix degradation, while the percentage of extravasation is still comparable between conditions due to protection of the endothelium barrier. This result validates our platforms capability for allowing inter-cell population signaling between channels, and permitting an extravasation response. Furthermore, our results agree with previous findings [9, 44], and supports the need to investigate osteoclast secreted factors for potential new drug therapies.

When the effects of OFF-stimulated osteocytes on breast cancer extravasation was investigated (group II), we observed a significant reduction in extravasation distance and percentage compared to static osteocytes (Fig. 5B). The reduced extravasation distance agrees with our previous finding, where CM from osteocytes exposed to flow reduced cancer trans-endothelial migration [18]. Mechanically stimulated osteocytes are known to increase adenosine triphosphate (ATP) secretion, through activation of gap junction hemichannels [51], and decrease RANKL release [27], which could both inhibit breast cancer migration [52, 53]. Furthermore, the application of flow reduces osteocyte apoptosis [54], which reduces IL-6 expression [55], a factor that stimulates cancer cell expression of MMP's [56, 57]. Previously, we observed that conditioned media from endothelial cells exposed to signals produced by flow-stimulated osteocytes significantly reduced the bone-metastatic breast cancer cells' gene expression of MMP-9 and frizzled-4 (FZD4), which are known to be involved in the cellular response, signaling, and locomotion aspects of metastasis [19]. However, mechanical stimulation also up-regulates prostaglandin E2 (PGE-2) [58] and TGF-β1 [59] in osteocytes, both of which have been implicated in promoting metastasis through the increase of MMP expression in various cancers [60, 61]. Therefore, more specific investigation is needed in determining which of these factors are most important in regulating breakdown of the ECM. In terms of extravasation percentage, a significant reduction was observed when the MLO-Y4 cells were exposed to flow (Fig. 5B). This suggests signals generated by mechanically stimulated osteocytes are reducing extravasation through the endothelial barrier. This is potentially due to increased PGE-2 secretion by mechanically loaded MLO-Y4 cells [58], as PGE-2 is capable of enhancing the endothelial barrier and reducing endothelial permeability [62]. Further investigation is also needed to characterize this mechanism.

We finally investigated the direct effect of flow in the OCY channel on breast cancer extravasation by comparing two acellular conditions with or without flow (group III). No significant difference in extravasation distance and percentage were observed (Fig. 5C). Interestingly, it has been demonstrated that hydrostatic pressure applied to endothelial cells decreases VE-cadherin expression and destabilizes adherent junctions [63], and many studies have also shown that mechanical compression on cancer cells increases their ability to invade [64, 65], both of which should stimulate increased extravasation. We infer that the mechanical forces (e.g. pressure, fluid shear stresses) applied to the OCY channel aren't able to transduce through the side channel into the lumen and, therefore, this pro-metastatic effect is not observed. Based on this and our previous mass transport analysis using a similar microfluidic system [42], we believe transport of osteocyte signal is mainly diffusion regulated. More specifically, this model's implementation of hydrogel in the side channel would further minimize the convective mass transfer, which was already significantly reduced in our previous hydrogel-free platform [42].

While this microfluidic model provides significant improvements in terms of incorporating relevant mechanical stimuli to the bone metastatic environment, this model is not without limitations. For instance, this model lacks a relevant structural bone environment. *In vivo*, osteocytes reside within an

interconnected network called the lacunar-canalicular system, where they would experience modulated mechanotransduction due to differential attachments of various mechanosensors (such as the primary cilia, and tethering elements attached to cellular processes) [66–68]. However, both this work (Fig. 3B) and various 'macro' scaled models have demonstrated that osteocytes are able to generate relevant signaling in response to physiological levels of flow as is observed *in vivo* [27, 69]. Although the MLO-Y4 cells in our platform reside on a thin layer of collagen I instead of a physiological stiff structural bone environment, the stiff underlying substrate is still likely able to induce a physiological response [70, 71], unlike typical 3D hydrogel platforms where the cells are embedded within a soft substrate [72]. Furthermore, seeding osteocytes on collagen I coated glass slides is commonly used and validated in osteocyte mechanobiology studies [73].

Another limitation of this model is the potential variability in the shear stresses applied to the cells. Although the model fits the experimental data well across numerous device parameters, it still miscalculated shear stresses by approximately 20% (Fig. 3A). This flow system is sensitive to changes in channel heights, and this lack of flow accuracy could be accounted for by variations in channel heights that are common in SU-8 based microfabrication. This variability could be reduced by using more consistent microfabrication techniques, like hot embossing or micro milling.

Furthermore, the density of MDA-MB-231 cells injected to the lumen is much higher than the amount of circulating tumor cells (CTCs) present physiologically [74]. Nevertheless, as our focus is on the extravasation after adhesion, having an elevated extravasation baseline due to the numerous cancer cells helps us to investigate the impact of MLO-Y4 cell signaling. We are also using a mixture of rat-tail collagen I and Matrigel® to represent the ECM. Although Type I collagen is the main component of the bone matrix, the addition of Matrigel® here resembles the endothelial basement membrane, enhances vascular endothelium growth, and provides relevant growth factors found within bone matrix [75].

Lastly, use of combination of mouse-derived and human cell lines, as well as cell lines from the bone and umbilical cord environments may raise concerns on the across-species variation. However, MDA-MB-231 cells are widely used in mouse models [76–79], and HUVECs are often used to represent the endothelium in breast cancer bone metastasis studies [31, 80, 81]. Using these cell lines in our study allows us to compare our work with work previously published in the literature. The use of established cell lines, such as the MLO-Y4 cells that are the most studied and characterized cell line for investigating osteocyte mechanobiology [73, 82], also provides better control of experiments with less uncertainty and variability. Additionally, although the MLO-Y4 cell line is known to not express certain signals characteristic of primary osteocytes [83, 84], the use of cell lines can be beneficial in terms of producing general treatment recommendations, as opposed to specific results obtained from patient-provided primary cells. Moreover, an advantage of this microfluidic platform is that it could eventually incorporate primary osteocytes, which are difficult to isolate and terminally differentiated [83], making them non-viable for macro-scaled experiments.

In this study we established a new tool for investigating osteocyte-regulated breast cancer bone metastasis through mechanical stimulation. This device will support future investigation in the specific mechanisms underlying bone loading regulation of bone metastasis, and testing the effect of specific drugs for mitigating the risks of bone metastasis. One of the potential directions we could investigate will be the suppression of MMPs expression due to soluble factors secreted by mechanically stimulated MLO-Y4 cells, such as PGE-2 and TGF-β1. Additionally, we could investigate VE-cadherin function and permeability regulation by flow-induced osteocyte signaling. As well, this device could be used as a model for other types of cancer metastasis to bone, or other organs undergoing mechanical stimulation, such as the lung. Furthermore, the integration of on-chip biosensors as our long-term goal could allow for real-time investigation of various cellular factors involved in the metastatic process [85], quantitative measurement of cancer invasion [86], as well as modifications in endothelial permeability through electrical impedance measurements [87, 88].

In summary, we developed a novel microfluidic platform for the study of breast cancer extravasation in bone through a relevant and cellularized 3D microfluidic tissue *in vitro*. This device enables the integration of physiologically relevant bone fluid flow stimulation and real-time intercellular signaling between three different cell-types. Using this platform, we confirmed previous results obtained by our lab that suggest mechanically stimulated osteocytes inhibited transendothelial breast cancer extravasation. This platform can provide insights into the role of fluid-based mechanoregulation of various metastatic cancers in a more relevant tissue environment than typical *in vitro* studies and help bridge the gap between *in vitro* and *in vivo* experimentation in the bone metastasis field.

Supplementary data

Supplementary data is available at *INTBIO* online.

Acknowledgments

We acknowledge Akash Chauhan and Ruihe (Bolt) Zhang for machining the microfluidic pump frame. Funding for this research was provided by the National Sciences and Engineering Research Council (NSERC).

References

1. Lipton A, Uzzo R, Amato RJ et al. The science and practice of bone health in oncology: managing bone loss and metastasis in patients with solid tumors. *J Natl Compr Canc Netw* 2009;**7**:S1–29.
2. Brunetti G, Colaianni G, Faienza MF et al. Osteotropic cancers: from primary tumor to bone. *Clin. Rev. Bone Miner. Metab*. 2013;**11**:94–102.
3. Brunetti G, Di Benedetto A, Mori G. Bone remodeling. Imaging Prosthet. Joints A Comb. Radiol. Clin. Perspect. p. 27–37, 2014.
4. Chen Y-C, Sosnoski DM, Mastro AM. Breast cancer metastasis to the bone: mechanisms of bone loss. *Breast Cancer Res* 2010;**12**:215.
5. Liu S, Fan Y, Chen A et al. Osteocyte-driven downregulation of snail restrains effects of Drd2 inhibitors on mammary tumor cells. *Cancer Res* 2018;**78**:3865–76.
6. Gdowski AS, Ranjan A, Vishwanatha JK. Current concepts in bone metastasis, contemporary therapeutic strategies and ongoing clinical trials. *J Exp Clin Cancer Res* 2017;**36**:1–13.

7. Sheill G, Guinan EM, Peat N et al. Considerations for exercise prescription in patients with bone metastases: a comprehensive narrative review. *PM R* 2018;**10**:843–64.
8. Lynch ME, Brooks D, Monahan S et al. In vivo tibial compression decreases osteolysis and tumour formation in a human metastatic breast cancer model. *J Bone Miner Res* 2013;**28**:2357–67.
9. Le Pape F, Vargas G, Clézardin P. The role of osteoclasts in breast cancer bone metastasis. *J Bone Oncol* 2016;**5**:93–5.
10. Guise TA, Yin JJ, Mohammad KS. Role of endothelin-1 in osteoblastic bone metastases. *Cancer* 2003;**97**:779–84.
11. Reymond N, D'Água BB, Ridley AJ. Crossing the endothelial barrier during metastasis. *Nat Rev Cancer* 2013;**13**:858–70.
12. Glinsky VV. Intravascular cell-to-cell adhesive interactions and bone metastasis. *Cancer Metastasis Rev* 2006;**25**:531–40.
13. Miles FL, Pruitt FL, Van Golen KL et al. Stepping out of the flow: capillary extravasation in cancer metastasis. *Clin Exp Metastasis* 2008;**25**:305–24.
14. Aragon-Sanabria V, Pohler SE, Eswar VJ et al. VE-Cadherin disassembly and cell contractility in the endothelium are necessary for barrier disruption induced by tumor cells. *Sci Rep* 2017;**7**:1–15.
15. Paschos KA, Canovas D, Bird NC. The role of cell adhesion molecules in the progression of colorectal cancer and the development of liver metastasis. *Cell. Signal* 2009;**21**:665–74.
16. Sottnik JL, Dai J, Zhang H et al. Tumor-induced pressure in the bone microenvironment causes osteocytes to promote the growth of prostate cancer bone metastases. *Cancer Res* 2015;**75**:2151–58.
17. Qiao H, Cui Z, Yang S et al. Targeting osteocytes to attenuate early breast cancer bone metastasis by theranostic upconversion nanoparticles with responsive plumbagin release. *ACS Nano* 2017;**11**:7259–73.
18. Ma Y-HV, Lam C, Dalmia S et al. Mechanical regulation of breast cancer migration and apoptosis via direct and indirect osteocyte signaling. *J. Cell. Biochem* 2018;**119**:5665–75.
19. Ma Y-HV, Xu L, Mei X et al. Mechanically stimulated osteocytes reduce the bone-metastatic potential of breast cancer cells in vitro by signaling through endothelial cells. *J Cell Biochem* 2019;**120**:7590–7601.
20. Cheung W-Y, Liu C, Tonelli-Zasarsky RML et al. Osteocyte apoptosis is mechanically regulated and induces angiogenesis in vitro. *J Orthop Res* 2011;**29**:523–30.
21. Prasadam I, Zhou Y, Du Z et al. Osteocyte-induced angiogenesis via VEGF–MAPK-dependent pathways in endothelial cells. *Mol Cell Biochem* 2014;**386**:15–25.
22. Xiong J, Piemontese M, Onal M et al. Osteocytes, not osteoblasts or lining cells, are the main source of the RANKL required for osteoclast formation in remodeling bone. *PLoS One* 2015;**10**:e0138189.
23. Lau E, Al-Dujaili S, Guenther A et al. Effect of low-magnitude, high-frequency vibration on osteocytes in the regulation of osteoclasts. *Bone* 2010;**46**:1508–15.
24. Hao Z, Ma Y, Wu J et al. Osteocytes regulate osteoblast differentiation and osteoclast activity through Interleukin-6 under mechanical loading. *RSC Adv* 2017;**7**:50200–09.
25. Taylor AF, Saunders MM, Shingle DL et al. Mechanically stimulated osteocytes regulate osteoblastic activity via gap junctions. *Am J Physiol Cell Physiol* 2006;**292**:C545–52.
26. Klein-Nulend J, Bacabac RG, Bakker AD. Mechanical loading and how it affects bone cells: the role of the osteocyte cytoskeleton in maintaining our skeleton. *Eur Cell Mater* 2012;**24**:278–91.
27. You L, Temiyasathit S, Lee P et al. Osteocytes as mechanosensors in the inhibition of bone resorption due to mechanical loading. *Bone* 2008;**42**:172–9.
28. Bonewald LF. The amazing osteocyte. *J Bone Miner Res* 2011;**26**:229–38.
29. Chen MB, Whisler JA, Jeon JS et al. Mechanisms of tumor cell extravasation in an in vitro microvascular network platform. *Integr Biol (Camo)* 2013;**5**:1262–71.
30. Zhang Q, Liu T, Qin J. A microfluidic-based device for study of transendothelial invasion of tumor aggregates in real-time. *Lab Chip* 2012;**12**:2837–42.
31. Bersini S, Jeon JS, Dubini G et al. A microfluidic 3D in vitro model for specificity of breast cancer metastasis to bone. *Biomaterials* 2014;**35**:2454–61.
32. Jeon JS, Bersini S, Gilardi M et al. Human 3D vascularized organotypic microfluidic assays to study breast cancer cell extravasation. *Proc Natl Acad Sci USA* 2015;**112**:214–9.
33. Young EWK. Cells, tissues, and organs on chips: challenges and opportunities for the cancer tumor microenvironment. *Integr Biol (Camb)* 2013;**5**:1096.
34. Zervantonakis IK, Hughes-Alford SK, Charest JL et al. Three-dimensional microfluidic model for tumor cell intravasation and endothelial barrier function. *Proc Natl Acad Sci USA* 2012;**109**:13515–20.
35. Chaw KC, Manimaran M, Tay EH et al. Multi-step microfluidic device for studying cancer metastasis. *Lab Chip* 2007;**7**:1041–7.
36. Marturano-Kruik A, Nava MM, Yeager K et al. Human bone perivascular niche-on-a-chip for studying metastatic colonization. *Proc Natl Acad Sci USA* 2018;**115**:1256–61.
37. Weinbaum S, Cowin SC, Zeng Y. A model for the excitation of osteocytes by mechanical loading-induced bone fluid shear stresses. *J Biomech* 1994;**27**:339–60.
38. Mi LY, Fritton SP, Basu M et al. Analysis of avian bone response to mechanical loading-Part one: Distribution of bone fluid shear stress induced by bending and axial loading. *Biomech Model Mechanobiol* 2005;**4**:118–31.
39. Price C, Zhou X, Li W et al. Real-time measurement of solute transport within the lacunar-canalicular system of mechanically loaded bone: Direct evidence for load-induced fluid flow. *J Bone Miner Res* 2011;**26**:277–85.
40. Jing D, Baik AD, Lu XL et al. In situ intracellular calcium oscillations in osteocytes in intact mouse long bones under dynamic mechanical loading. *FASEB J* 2014;**28**:1582–92.
41. Liu C, Zhao Y, Cheung W-Y et al. Effects of cyclic hydraulic pressure on osteocytes. *Bone* 2010;**46**:1449–56.
42. Middleton K, Al-Dujaili S, Mei X et al. Microfluidic co-culture platform for investigating osteocyte-osteoclast signalling during fluid shear stress mechanostimulation. *J Biomech* 2017;**59**:35–42.
43. Bischel LL, Young EWK, Mader BR et al. Tubeless microfluidic angiogenesis assay with three-dimensional endothelial-lined microvessels. *Biomaterials* 2013;**34**:1471–7.
44. Krzeszinski JY, Schwaid AG, Cheng WY et al. Lipid osteoclastokines regulate breast cancer bone metastasis. *Endocrinology* 2018;**158**:477–89.
45. Zhang J, Lu A, Beech D et al. Suppression of breast cancer metastasis through the inhibition of VEGF-mediated tumor angiogenesis. *Cancer Ther* 2007;**5**:273–86.
46. Kiesel L, Kohl A. Role of the RANK/RANKL pathway in breast cancer. *Maturitas* 2016;**86**:10–6.
47. Ryu J, Kim HJ, Chang EJ et al. Sphingosine 1-phosphate as a regulator of osteoclast differentiation and osteoclast-osteoblast coupling. *EMBO J* 2006;**25**:5840–51.

48. Sarkar S, Maceyka M, Hait NC et al. Sphingosine kinase 1 is required for migration, proliferation and survival of MCF-7 human breast cancer cells. *FEBS Lett* 2005;**579**:5313–7.
49. Kim E-S, Kim J-S, Kim SG et al. Sphingosine 1-phosphate regulates matrix metalloproteinase-9 expression and breast cell invasion through S1P3-G q coupling. *J Cell Sci* 2011;**124**:2220–30.
50. Xiong Y, Hla T. Sphingosine-1-Phosphate Signaling in Immunology and Infectious Diseases. In: Oldstone MBA, Rosen H (eds). *Curr Top Microbiol Immunol*. Cham: Springer International Publishing, 2014, 85–105.
51. Genetos DC, Kephart CJ, Zhang Y et al. Oscillating fluid flow activation of gap junction hemichannels induces ATP release from MLO-Y4 osteocytes. *J Cell Physiol* 2007;**212**:207–14.
52. Zhou JZ, Riquelme MA, Gao X et al. Differential impact of adenosine nucleotides released by osteocytes on breast cancer growth and bone metastasis. *Oncogene* 2014;**34**:1831–42.
53. Jones DH, Nakashima T, Sanchez OH et al. Regulation of cancer cell migration and bone metastasis by RANKL. *Nature* 2006;**440**:692–6.
54. Cheung W-YY, Liu C, Tonelli-Zasarsky RML et al. Osteocyte apoptosis is mechanically regulated and induces angiogenesis in vitro. *J Orthop Res* 2011;**29**:523–30.
55. Cheung W-YY, Simmons CA, You L. Osteocyte apoptosis regulates osteoclast precursor adhesion via osteocytic IL-6 secretion and endothelial ICAM-1 expression. *Bone* 2012;**50**:104–10.
56. Banach A, Chen J, Liu A et al. Interleukin-6 increases matrix metalloproteinase-14 (MMP-14) levels via down-regulation of p53 to drive cancer progression. *Oncotarget* 2016;**7**:61107–20.
57. Mohamed MM, El-Ghonaimy EA, Mahana N et al. Hormonal-receptor positive breast cancer: IL-6 augments invasion and lymph node metastasis via stimulating cathepsin B expression. *J Adv Res* 2016;**7**:661–70.
58. Zhang JN, Zhao Y, Liu C et al. The role of the sphingosine-1-phosphate signaling pathway in osteocyte mechanotransduction. *Bone* 2015;**79**:71–8.
59. Heino TJ, Hentunen TA, Kalervo Vnnen H. Osteocytes inhibit osteoclastic bone resorption through transforming growth factor-β: Enhancement by estrogen. *J Cell Biochem* 2002;**85**:185–97.
60. Itatsu K, Sasaki M, Yamaguchi J et al. Cyclooxygenase-2 is involved in the up-regulation of matrix metalloproteinase-9 in cholangiocarcinoma induced by tumor necrosis factor-α. *Am. J. Pathol* 2009;**174**:829–41.
61. Sun L, Ananthanarayan V, Ottaviano AJ et al. Transforming growth factor-1 promotes matrix metalloproteinase-9-mediated oral cancer invasion through snail expression. *Mol Cancer Res* 2008;**6**:10–20.
62. Birukova AA, Zagranichnaya T, Fu P et al. Prostaglandins PGE2 and PGI2 promote endothelial barrier enhancement via PKA- and Epac1/Rap1-dependent Rac activation. *Exp Cell Res* 2007;**313**:2504–20.
63. Ohashi T, Sugaya Y, Sakamoto N et al. Hydrostatic pressure influences morphology and expression of VE-cadherin of vascular endothelial cells. *J Biomech* 2007;**40**:2399–2405.
64. Polacheck WJ, Charest JL, Kamm RD. Interstitial flow influences direction of tumor cell migration through competing mechanisms. *Proc Natl Acad Sci USA* 2011;**108**:11115–20.
65. Tse JM, Cheng G, Tyrrell JA et al. Mechanical compression drives cancer cells toward invasive phenotype. *Proc Natl Acad Sci USA* 2012;**109**:911–6.
66. You LD, Weinbaum S, Cowin SC et al. Ultrastructure of the osteocyte process and its pericellular matrix. *Anat Rec A Discov Mol Cell Evol Biol* 2004;**278**:505–13.
67. McNamara LM, Majeska RJ, Weinbaum S et al. Attachment of osteocyte cell processes to the bone matrix. *Anat Rec (Hoboken)* 2009;**292**:355–63.
68. Malone AMD, Anderson CT, Tummala P et al. Primary cilia mediate mechanosensing in bone cells by a calcium-independent mechanism. *Proc Natl Acad Sci USA* 2007;**104**:13325–30.
69. Lu L, Huo B, Park M et al. Calcium response in osteocytic networks under steady and oscillatory fluid flow. *Bone* 2012;**51**:466–73.
70. Plant AL, Bhadriraju K, Spurlin TA et al. Cell response to matrix mechanics: focus on collagen. *Biochim. Biophys. Acta - Mol. Cell Res* 2009;**1793**:893–902.
71. Mullen CA, Vaughan TJ, Billiar KL et al. The effect of substrate stiffness, thickness, and cross-linking density on osteogenic cell behavior. *Biophys J* 2015;**108**:1604–12.
72. Buxboim A, Rajagopal K, Brown AEX et al. How deeply cells feel: methods for thin gels. *J Phys Condens Matter* 2011;**22**:194116.
73. Uda Y, Azab E, Sun N et al. Osteocyte mechanobiology. *Curr Osteoporos Rep* 2017;**15**:318–25.
74. Yu M, Stott S, Toner M et al. Circulating tumor cells: approaches to isolation and characterization. *J Cell Biol* 2011;**192**:373–82.
75. Florencio-silva R, Sasso G, Sasso-cerri E et al. Biology of bone tissue: structure, function, and factors that influence bone cells. *Biomed Res Int* 2015;**2015**:1–17.
76. Iorns E, Drews-Elger K, Ward TM et al. A new mouse model for the study of human breast cancer metastasis. *PLoS One* 2012;**7**:e47995.
77. Wright LE, Ottewell PD, Rucci N et al. Murine models of breast cancer bone metastasis. *Bonekey Rep* 2016;**5**:1–11.
78. Kim JB, O'Hare MJ, Stein R. Models of breast cancer: is merging human and animal models the future? *Breast Cancer Res* 2004;**6**:22–30.
79. Fantozzi A, Christofori G. Mouse models of breast cancer metastasis. *Breast Cancer Res* 2006;**8**:212.
80. Marlow R, Honeth G, Lombardi S et al. A novel model of dormancy for bone metastatic breast cancer cells. *Cancer Res* 2013;**73**:6886–99.
81. Bray LJ, Secker C, Murekatete B et al. Three-dimensional in vitro hydro-and cryogel-based cell-culture models for the study of breast-cancer metastasis to bone. *Cancers (Basel)* 2018;**10**:E292.
82. Kato Y, Windle JJ, Koop BA et al. Establishment of an osteocyte-like cell line, MLO-Y4. *J Bone Miner Res* 2010;**12**:2014–23.
83. Kato Y, Windle JJ, Koop BA et al. Establishment of an osteocyte-like cell line, MLO-Y4. *J Bone Miner Res* 1997;**12**:2014–23.
84. Yang W, Harris MA, Heinrich JG et al. Gene expression signatures of a fibroblastoid preosteoblast and cuboidal osteoblast cell model compared to the MLO-Y4 osteocyte cell model. *Bone* 2009;**44**:32–45.
85. Son KJ, Gheibi P, Stybayeva G et al. Detecting cell-secreted growth factors in microfluidic devices using bead-based biosensors. *Microsyst Nanoeng* 2017;**3**:17025.
86. Lei KF, Tseng HP, Lee CY et al. Quantitative Study Of Cell Invasion Process Under Extracellular Stimulation Of Cytokine In A Microfluidic Device. *Sci Rep* 2016;**6**:6–13.
87. Young EWK, Watson MWL, Srigunapalan S et al. Technique for real-time measurements of endothelial permeability in a microfluidic membrane chip using laser-induced fluorescence detection. *Anal Chem* 2010;**82**:808–16.
88. Vogel PA, Halpin ST, Martin RS et al. Microfluidic transendothelial electrical resistance measurement device that enables blood flow and postgrowth experiments. *Anal Chem* 2011;**83**:4296–4301.